CROSS SECTIONS AND AMPLITUDES FOR SOFT INTERACTIONS AT THE LHC

Errol Gotsman
Tel Aviv University

(work done with Genya Levin and Uri Maor)

Background

- The classical Regge pole model a la' Donnachie and Landshoff provides a good description of soft hadron-hadron scattering upto the Tevatron energy.
  Disadvantages:
  1) Violates the Froissart-Martin bound.
  2) Underestimates cross sections for energies above that of the Tevatron.
- At the Tevatron energy we have a problem of different values of σ_{tot} measured by E710 and CDF Collaborations.
- At energies above $\sqrt{s} = 1800$ GeV, $\sigma_{tot} \sim ln^2 s$, "saturating" the Froissart-Martin bound.

Introduction

There are two types of models on the market today attempting to describe soft hadron-hadron scattering:

A

Models that work within a theoretical framework and calculate Elastic as well as Diffractive cross sections.

B

Models that assume a $ln^2 s$ behaviour for σ_{tot} and for σ_{inel}, and determine the strength of this term and other non-leading terms by comparing to data. Usually these are one channel models unable to calculate Diffractive cross sections.

- Prior to the publication of the LHC data, most model predictions for σ_{tot} at $\sqrt{s} = 1800$ GeV, were close to the E710 value of 72.1 ± 3.3 mb
- Following the publication of LHC data, revised models favour the CDF value of 80.03 ± 2.24 mb.
- In this talk I will concentrate on the GLM model and other models in group A.

Importance of Diffraction at the LHC

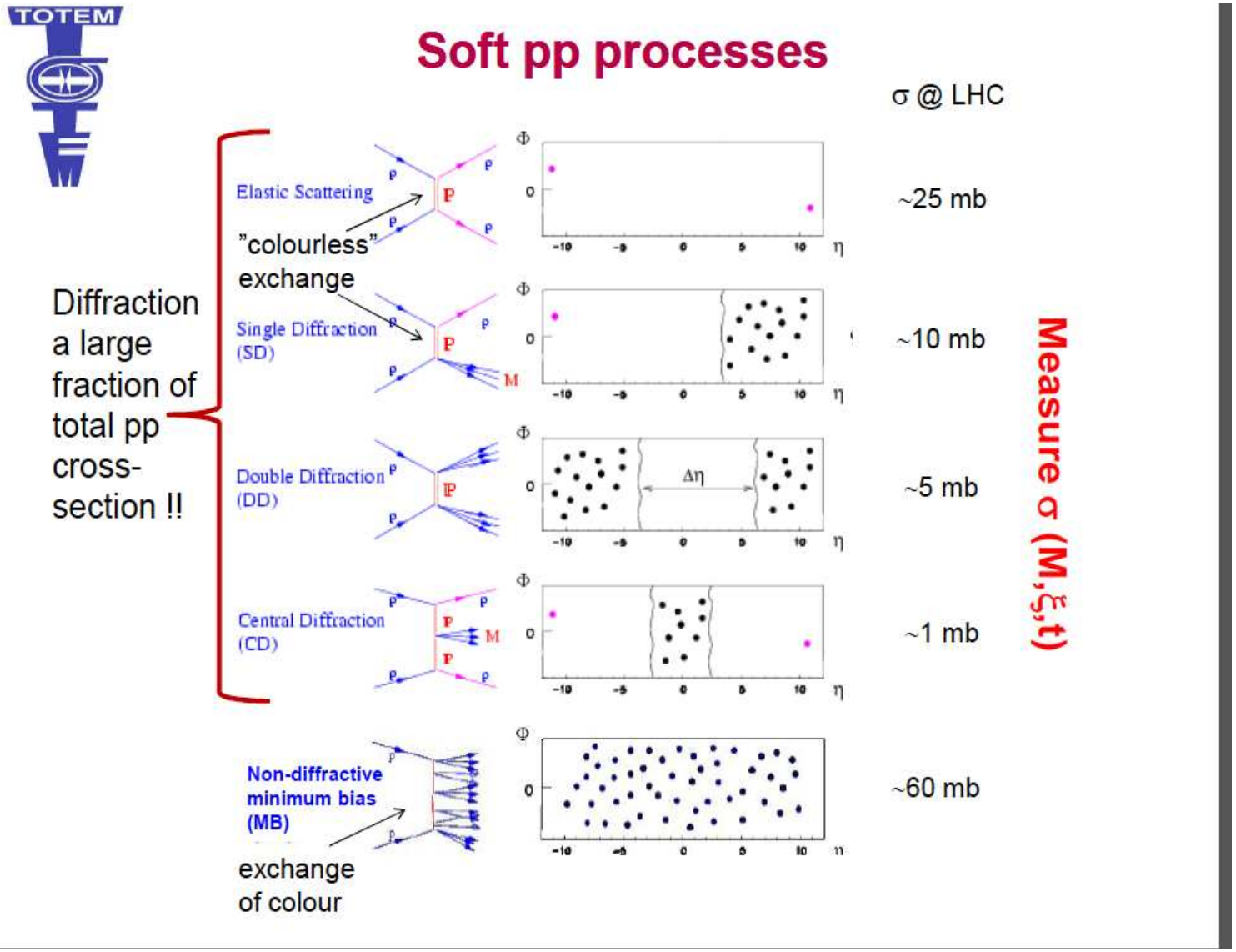

Good-Walker Formalism

The Good-Walker (G-W) formalism, considers the diffractively produced hadrons as a single hadronic state described by the wave function Ψ_D, which is orthonormal to the wave function Ψ_h of the incoming hadron (proton in the case of interest) i.e. $< \Psi_h | \Psi_D >= 0$.

One introduces two wave functions ψ_1 and ψ_2 that diagonalize the 2x2 interaction matrix $\mathbf{T}$

$$A_{i,k} =< \psi_i \, \psi_k | \mathbf{T} | \psi_{i'} \, \psi_{k'} >= A_{i,k} \, \delta_{i,i'} \, \delta_{k,k'}.$$

In this representation the observed states are written in the form

$$\psi_h = \alpha \, \psi_1 + \beta \, \psi_2 \, ,$$
$$\psi_D = -\beta \, \psi_1 + \alpha \, \psi_2$$
where, $\alpha^2 + \beta^2 = 1$

Good-Walker Formalism-2

The s-channel Unitarity constraints for (i,k) are analogous to the single channel equation:

$$Im\, A_{i,k}\,(s,b) = |A_{i,k}\,(s,b)\,|^2 + G^{in}_{i,k}(s,b),$$

$G^{in}_{i,k}$ is the summed probability for all non-G-W inelastic processes, including non-G-W "high mass diffraction" induced by multi-$I\!P$ interactions.

A simple solution to the above equation is:

$$A_{i,k}(s,b) = i\left(1-\exp\left(-\frac{\Omega_{i,k}(s,b)}{2}\right)\right), G^{in}_{i,k}(s,b) = 1-\exp\left(-\Omega_{i,k}(s,b)\right).$$

The opacities $\Omega_{i,k}$ are real, determined by the Born input.

Good-Walker Formalism-3

Amplitudes in two channel formalism are:

$$A_{el}(s,b) = i\{\alpha^4 A_{1,1} + 2\alpha^2\beta^2 A_{1,2} + \beta^4 A_{2,2}\},$$

$$A_{sd}(s,b) = i\alpha\beta\{-\alpha^2 A_{1,1} + (\alpha^2 - \beta^2) A_{1,2} + \beta^2 A_{2,2}\},$$

$$A_{dd}(s,b) = i\alpha^2\beta^2\{A_{1,1} - 2A_{1,2} + A_{2,2}\}.$$

With the G-W mechanism σ_{el} , σ_{sd} and σ_{dd} occur due to elastic scattering of ψ_1 and ψ_2, the correct degrees of freedom.

Since $A_{el}(s,b) = [1 - e^{-\Omega(s,b)/2}]$

the Opacity $\Omega_{el}(s,b) = -2ln[1 - A_{el}(s,b)]$

Examples of Pomeron diagrams

leading to diffraction NOT included in G-W mechanism

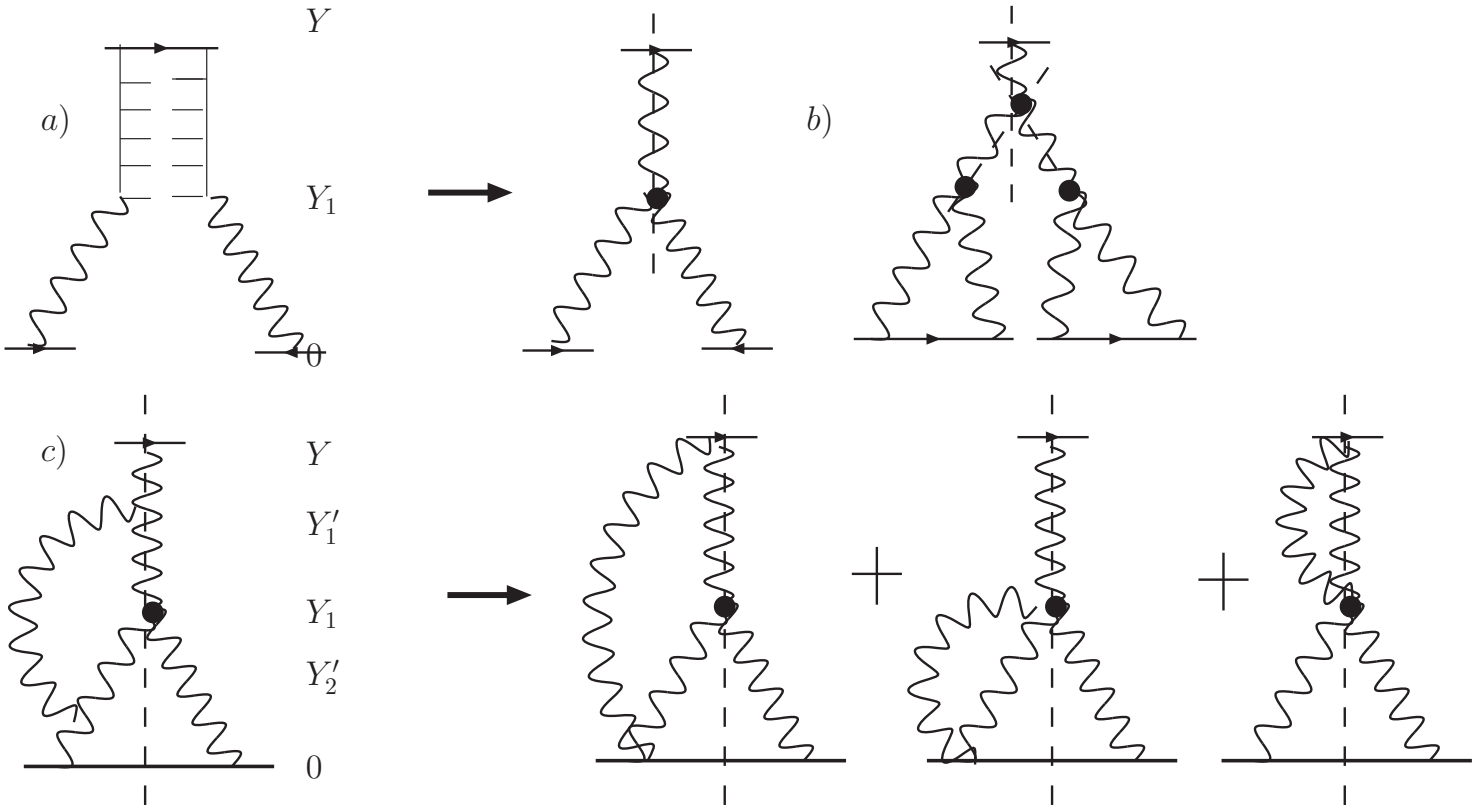

Examples of the Pomeron diagrams that lead to a different source of the diffractive dissociation that cannot be described in the framework of the G-W mechanism. (a) is the simplest diagram that describes the process of diffraction in the region of large mass $Y - Y_1 = \ln(M^2/s_0)$. (b) and (c) are examples of more complicated diagrams in the region of large mass. The dashed line shows the cut Pomeron, which describes the production of hadrons.

Example of enhanced and semi-enhanced diagram

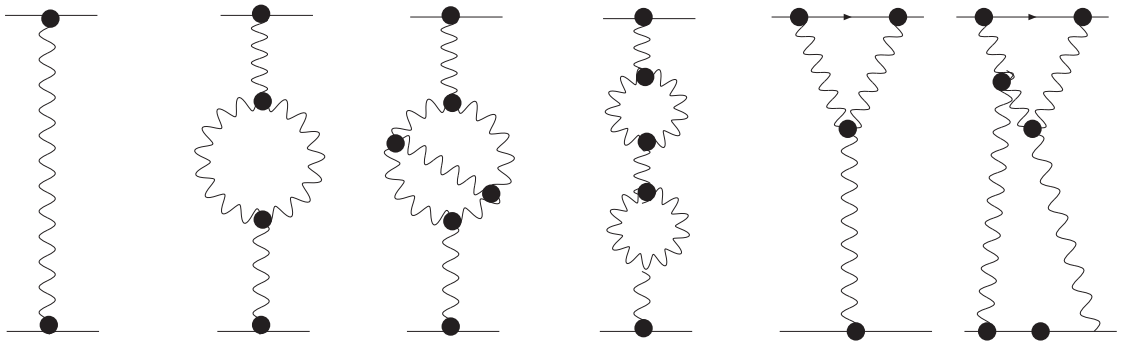

Different contributions to the Pomeron Green's function
a) examples of enhanced diagrams ;
(occur in the renormalisation of the Pomeron propagator)
b) examples of semi-enhanced diagrams
(occur in the renormalisation of the $I\!P$ -p vertex)
Multi-Pomeron interactions are crucial for the production of LARGE MASS DIFFRACTION

Our Formalism 1

The input opacity $\Omega_{i,k}(s,b)$ corresponds to an exchange of a single bare Pomeron.

$$\Omega_{i,k}(s,b) \;=\; g_i(b)\, g_k(b)\, P(s).$$

$P(s) \;=\; s^{\Delta_{I\!P}}$ and $g_i(b)$ is the Pomeron-hadron vertex parameterized in the form:

$$g_i\,(b) \;=\; g_i\, S_i(b) \;=\; \frac{g_i}{4\pi}\, m_i^3\, b\, K_1\,(m_i b)\,.$$

$S_i(b)$ is the Fourier transform of $\frac{1}{(1+q^2/m_i^2)^2}$, where, q is the transverse momentum carried by the Pomeron.

The Pomeron's Green function that includes all enhanced diagrams is approximated using the MPSI procedure, in which a multi Pomeron interaction (taking into account only triple Pomeron vertices) is approximated by large Pomeron loops of rapidity size of $\ln s$.
The Pomeron's Green Function is given by

$$G_{I\!P}\,(Y) \;=\; 1 \;-\; \exp\left(\frac{1}{T\,(Y)}\right)\, \frac{1}{T\,(Y)}\, \Gamma\left(0, \frac{1}{T\,(Y)}\right),$$

where $T\,(Y) \;=\; \gamma\, e^{\Delta_{I\!P} Y}$ and $\Gamma\,(0, 1/T)$ is the incomplete gamma function.

Fits to the Data

The parameters of our first fit GLM1 [EPJ C71,1553 (2011)] (prior to LHC) were determined by fitting to data
$20 \leq W \leq 1800$ GeV.

We had 58 data points and obtained a $\chi^2/d.f. \approx 0.86$.

This fit yields a value of $\sigma_{tot} = 91.2$ mb at W = 7 TeV.

Problem is that most data is at lower energies (W $\leq$ 500 GeV) and these have small errors, and hence have a dominant influence on the determination of the parameters.

To circumvent this we made another fit GLM2 [Phys.Rev. D85, 094007 (2012)] to data for energies W $>$ 500 GeV (including LHC), to determine the Pomeron parameters. We included 35 data points.

For the present version in addition we tuned the values of $\Delta_{I\!P}$, γ the Pomeron-proton vertex and the $G_{3I\!P}$ coupling, to give smooth cross sections over the complete energy range
$20 \leq W \leq$7000 GeV.

Values of Parameters for our updated version

$\Delta_{I\!P}$	β	$\alpha'_{I\!P}(GeV^{-2})$	$g_1\,(GeV^{-1})$	$g_2\,(GeV^{-1)}$	m_1 (GeV)	m_2 (GeV)
0.23	0.46	0.028	1.89	61.99	5.045	1.71
$\Delta_{I\!R}$	γ	$\alpha'_{I\!R}\,(GeV^{-2})$	$g_1^{I\!R}\,(GeV^{-1})$	$g_2^{I\!R}\,(GeV^{-1})$	$R^2_{0,1}\,(GeV^{-1})$	$G_{3I\!P}\,(GeV^{-1})$
- 0.47	0.0045	0.4	13.5	800	4.0	0.03

- $g_1(b)$ and $g_2(b)$ describe the vertices of interaction of the Pomeron with state 1 and state 2
- The Pomeron trajectory is $1 + \Delta_{I\!P} + \alpha'_{I\!P}$t
- γ denotes the low energy amplitude of the dipole-target interaction
- β denotes the mixing angle between the wave functions
- $G_{3I\!P}$ denotes the triple Pomeron coupling

Comparison of Elastic, SD and DD amplitudes at W = 7 TeV

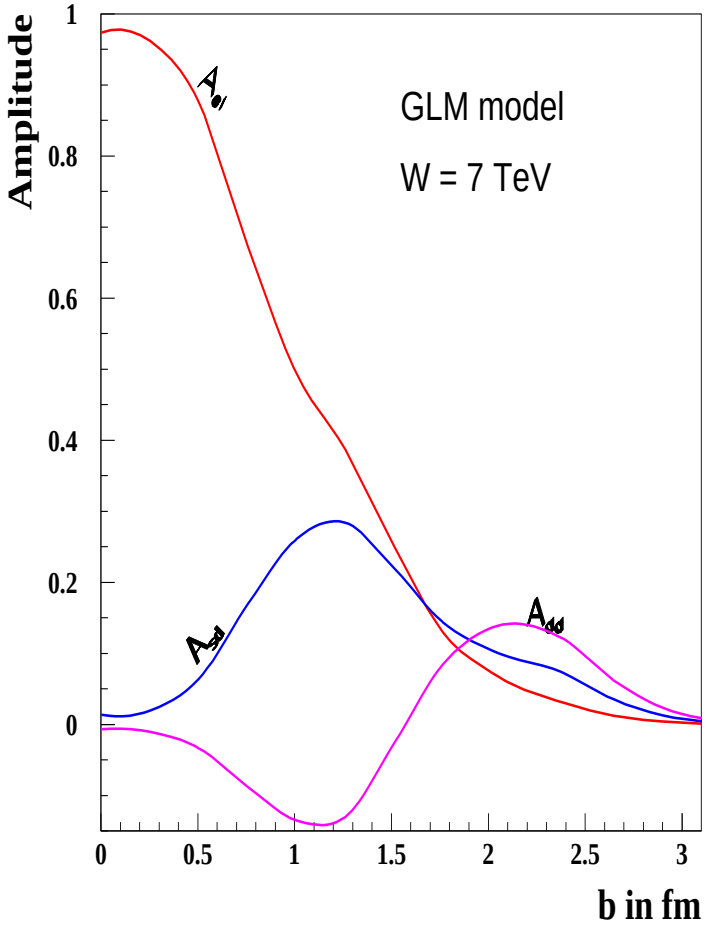

Note the completely different shapes of the three amplitudes, the elastic amplitude $A_{el}(b)$ is gaussian in shape, while the single diffractive amplitude $A_{sd}(b)$ and the double diffractive amplitude $A_{dd}(b)$ are very small at small b .

A_{el} has a peak is at b = 0 fm, A_{sd} peak is at 1.25 fm, while A_{dd}'s maximum is at b = 2.15 fm.

Elastic Amplitudes of the GLM model

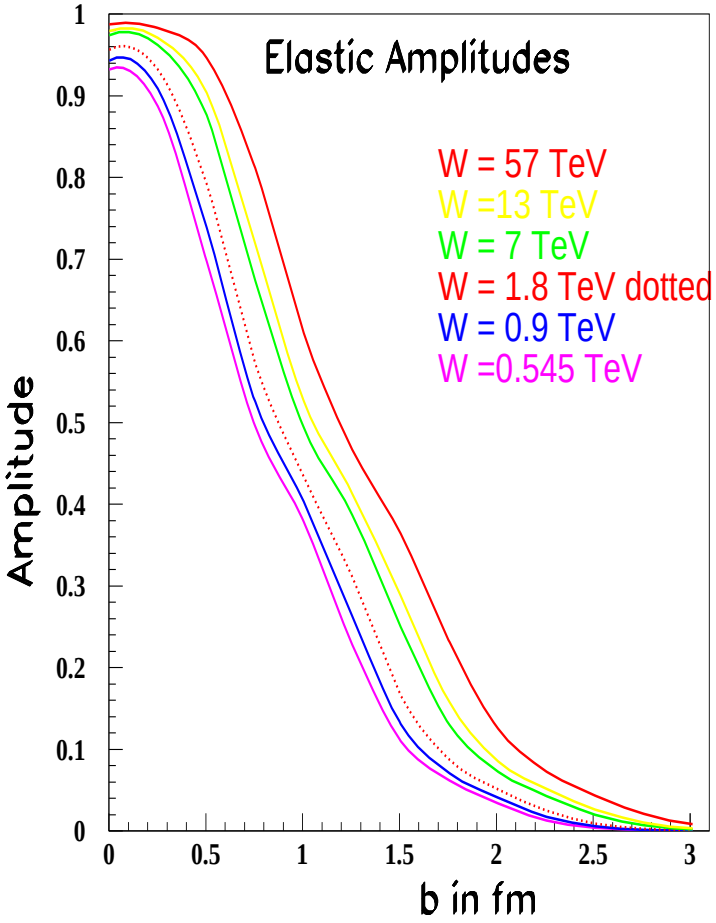

I) Note the overall gaussian shape of the elastic amplitudes for all energies $0.545 \leq W \leq 57$ TeV, with the width and height of the gaussian growing with increasing energy.

II) For small values of impact parameter b the slope of the amplitudes decreases with increasing energy.

III) The elastic amplitude (as $b \longrightarrow 0$) becomes almost flat for W $= 57$ TeV, where it is still below the Unitarity limit $A_{el} = 1$.

Single and Double Diffractive GW Amplitudes

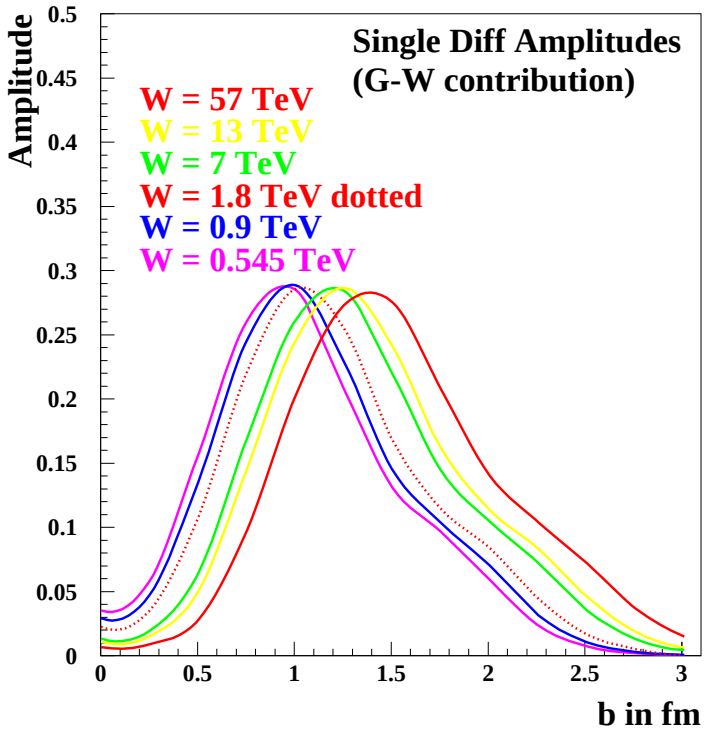

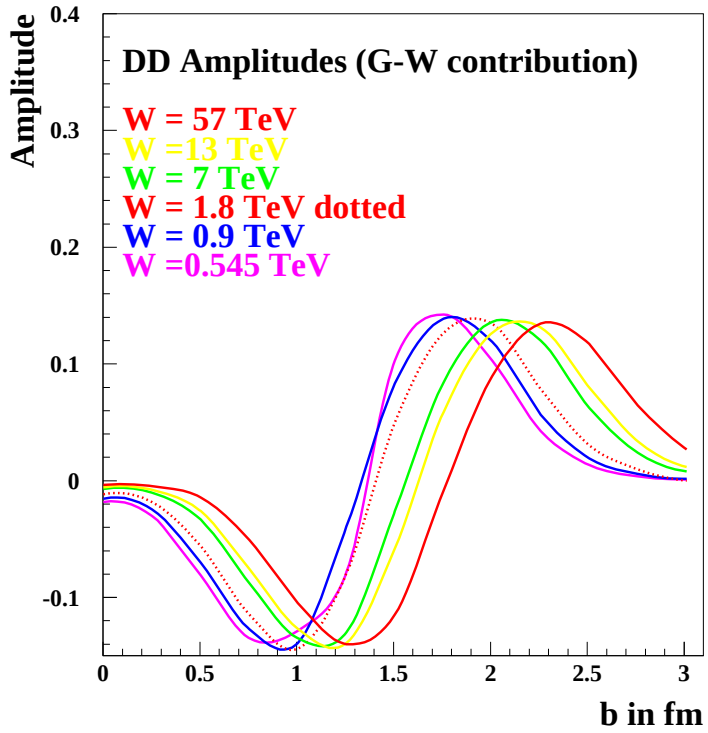

Common feature of both diffractive amplitudes is that with increasing energy the peaks broaden and become more peripheral.

RMK Eur.Phys.J. C72 (2012) 1937

Have attempted to extract the form of the Elastic Opacity directly from data:
Assuming that the Real part of the scattering amplitude is small:

$$\mathrm{Im}A(b) \;=\; \int \sqrt{\frac{d\sigma_{\mathrm{el}}}{dt}\frac{16\pi}{1+\rho^2}}\; J_0(q_t b)\; \frac{q_t dq_t}{4\pi}$$

where $q_t = \sqrt{|t|}$ and $\rho \equiv \mathrm{Re}A/\mathrm{Im}A$

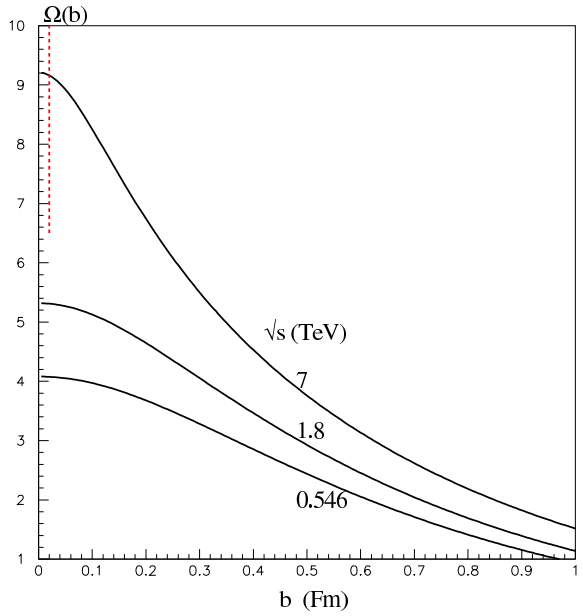

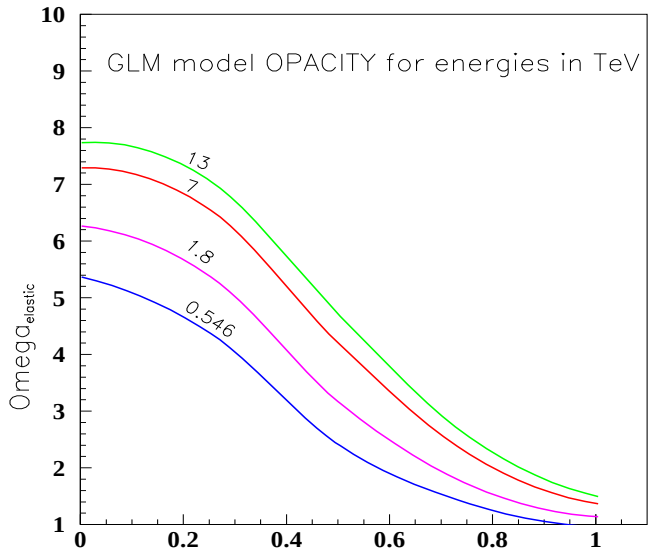

The proton opacity $\Omega(b)$ determined directly from the pp $d\sigma_{\mathrm{el}}/dt$ data at 546 GeV , 1.8 TeV and 7 TeV data.

The uncertainty on the LHC value at $b = 0$ is indicated by a dashed red line.

Comparison with FKK and KPPS parameterizations

FKK (Ferreira, Kohara and Kodama *Eur. Phys. J.* **C73**, 2326 (2013)).

KPPS (Kopeliovich, Potashnikova, Povh and Schmidt *Phys. Rev.* **D76**, 094020 (2007)).

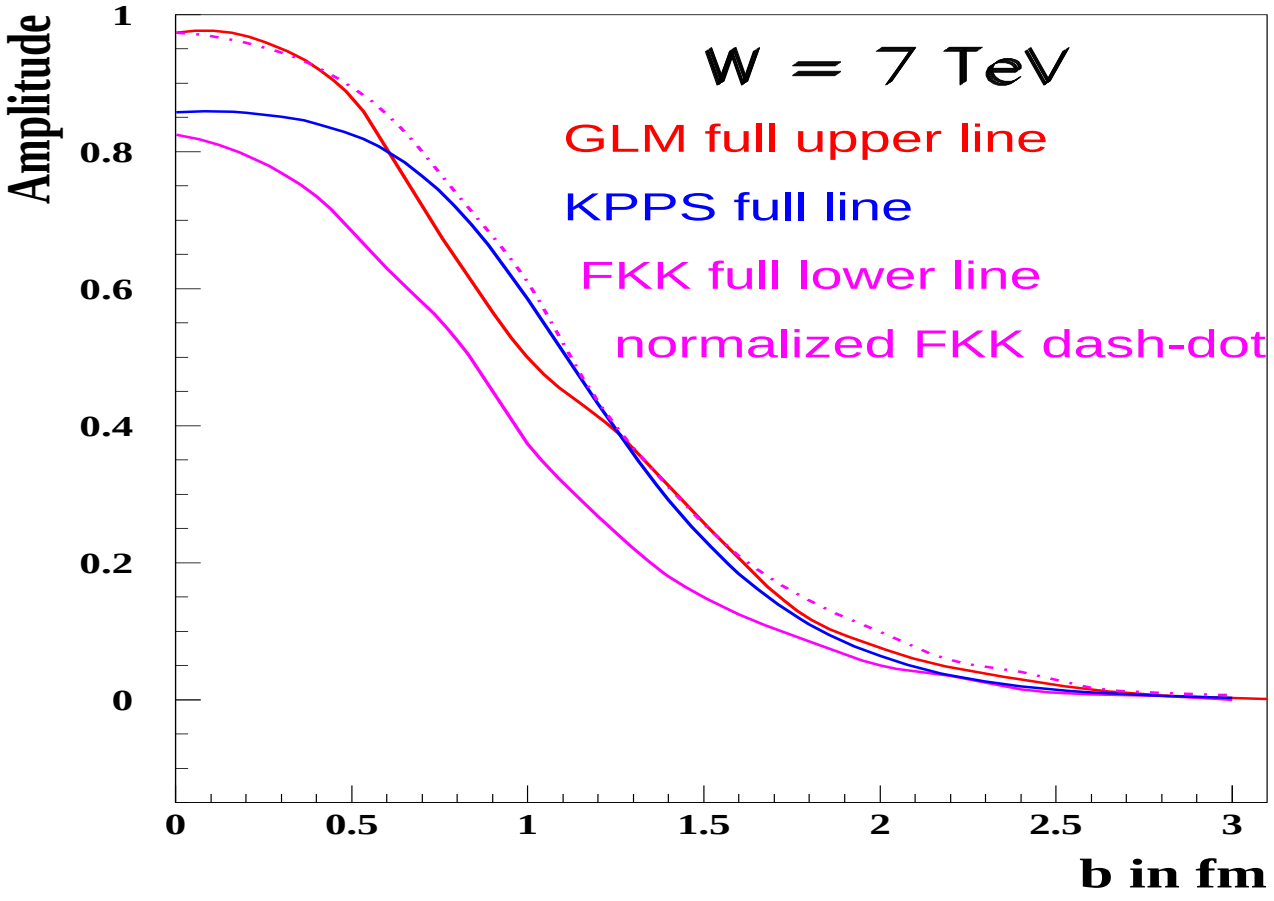

Comparison of DIPSY (including enhanced and semi-enhanced)

and GLM (only GW) S.D. amplitudes

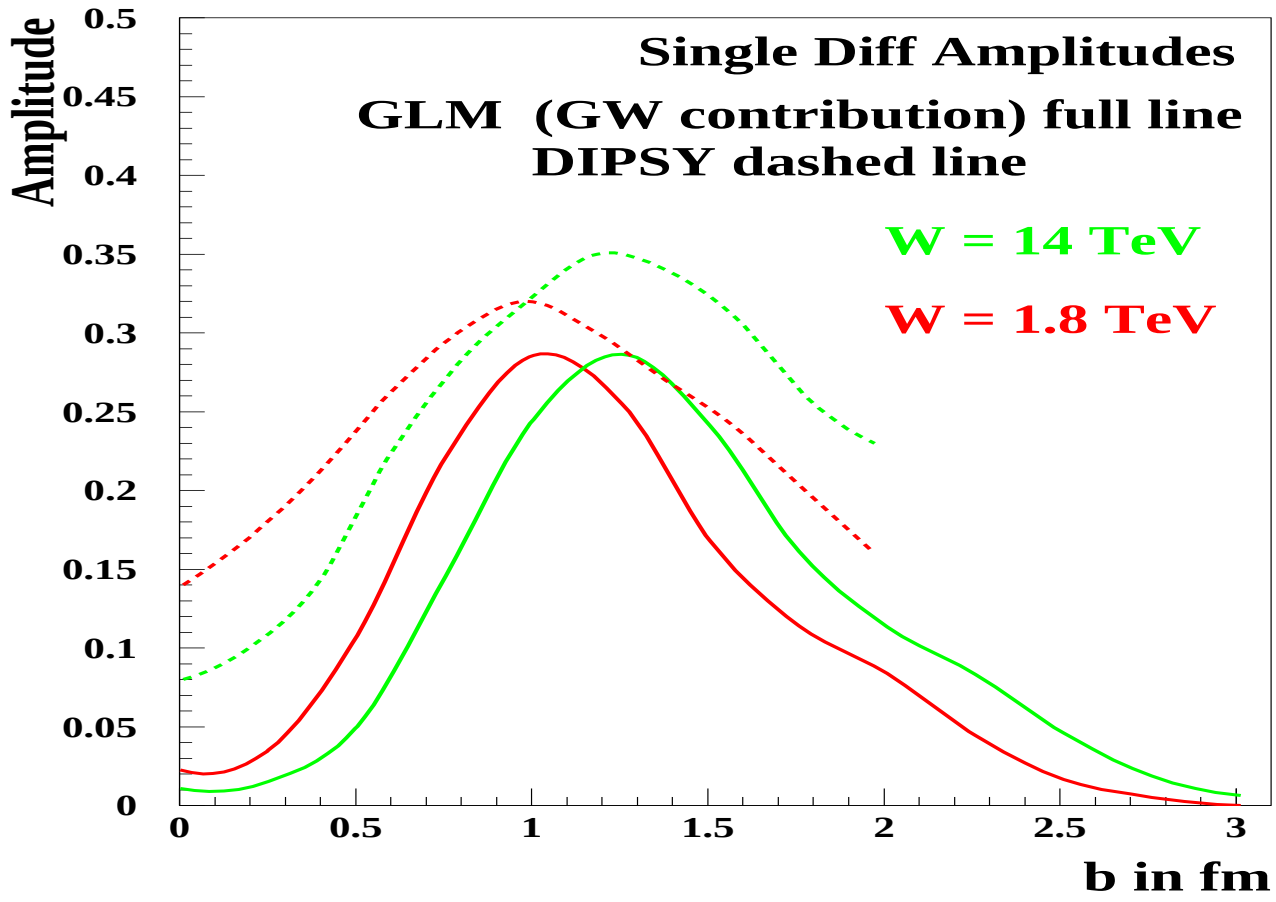

Results of GLM model

$\sqrt{s}$ TeV	1.8	7	8
σ_{tot} mb	79.2	98.6	101.
σ_{el} mb	18.5	24.6	25.2
$\sigma_{sd}(M \leq M_0)$ mb		$10.7 + (2.8)^{nGW}$	$10.9 + (2.89)^{nGW}$
$\sigma_{sd}(M^2 < 0.05s)mb$	$9.2+ (1.95)^{nGW}$	$10.7 + (4.18)^{nGW}$	$10.9 + (4.3)^{nGW}$
σ_{dd} mb	$5.12 + (0.38)^{nGW}$	$6.2 + (1.166)^{nGW}$	$6.32 + (1.29)^{nGW}$
$B_{el}\ GeV^{-2}$	17.4	20.2	20.4
$B_{sd}^{GW}\ GeV^{-2}$	6.36	8.01	8.15
σ_{inel} mb	60.7	74.	75.6
$\frac{d\sigma}{dt}\|_{t=0}\, mb/GeV^2$	326.34	506.4	530.7

$\sqrt{s}$ TeV	13	14	57
σ_{tot} mb	108.0	109.0	130.0
σ_{el} mb	27.5	27.9	34.8
$\sigma_{sd}(M^2 < 0.05s)$ mb	$11.4 +(5.56)^{nGW}$	$11.5 +(5.81)^{nGW}$	$13.0 + (8.68)^{nGW}$
σ_{dd} mb	$6.73 + (1.47)^{nGW}$	$6.78 + (1.59)^{nGW}$	$7.95 + (5.19)^{nGW}$
$B_{el}\ GeV^{-2}$	21.5	21.6	24.6
σ_{inel} mb	80.7	81.1	95.2
$\frac{d\sigma}{dt}\|_{t=0}\, mb/GeV^2$	597.6	608.11	879.2

Predictions of our model for different energies W. M_0 is taken to be equal to $200GeV$ as ALICE measured the cross section of the diffraction production with this restriction.

Comparison of the Energy Dependence of GLM and Experimental Data

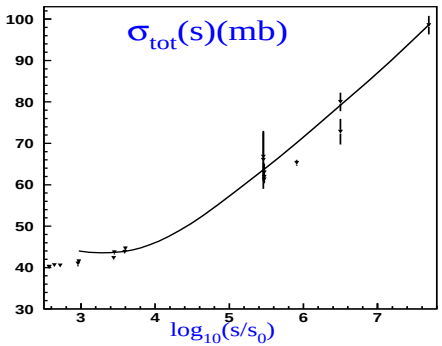

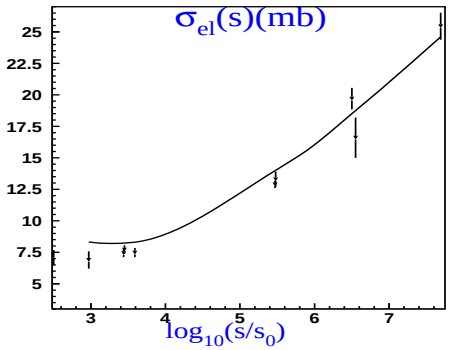

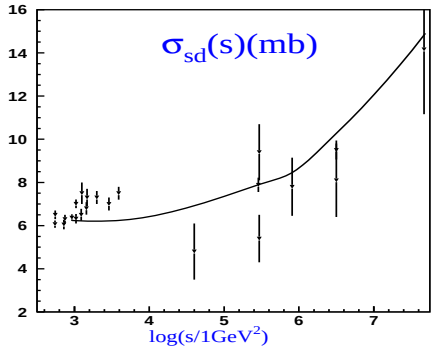

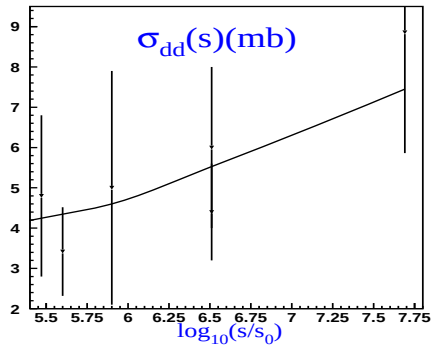

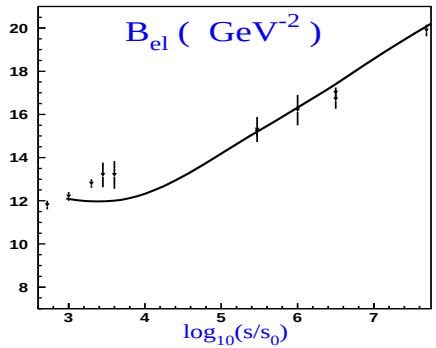

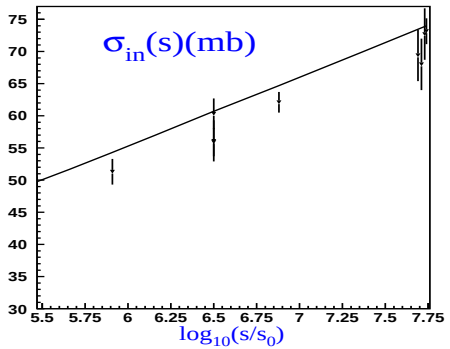

GLM Differential cross section and Experimental Data at 1.8 and 7 TeV

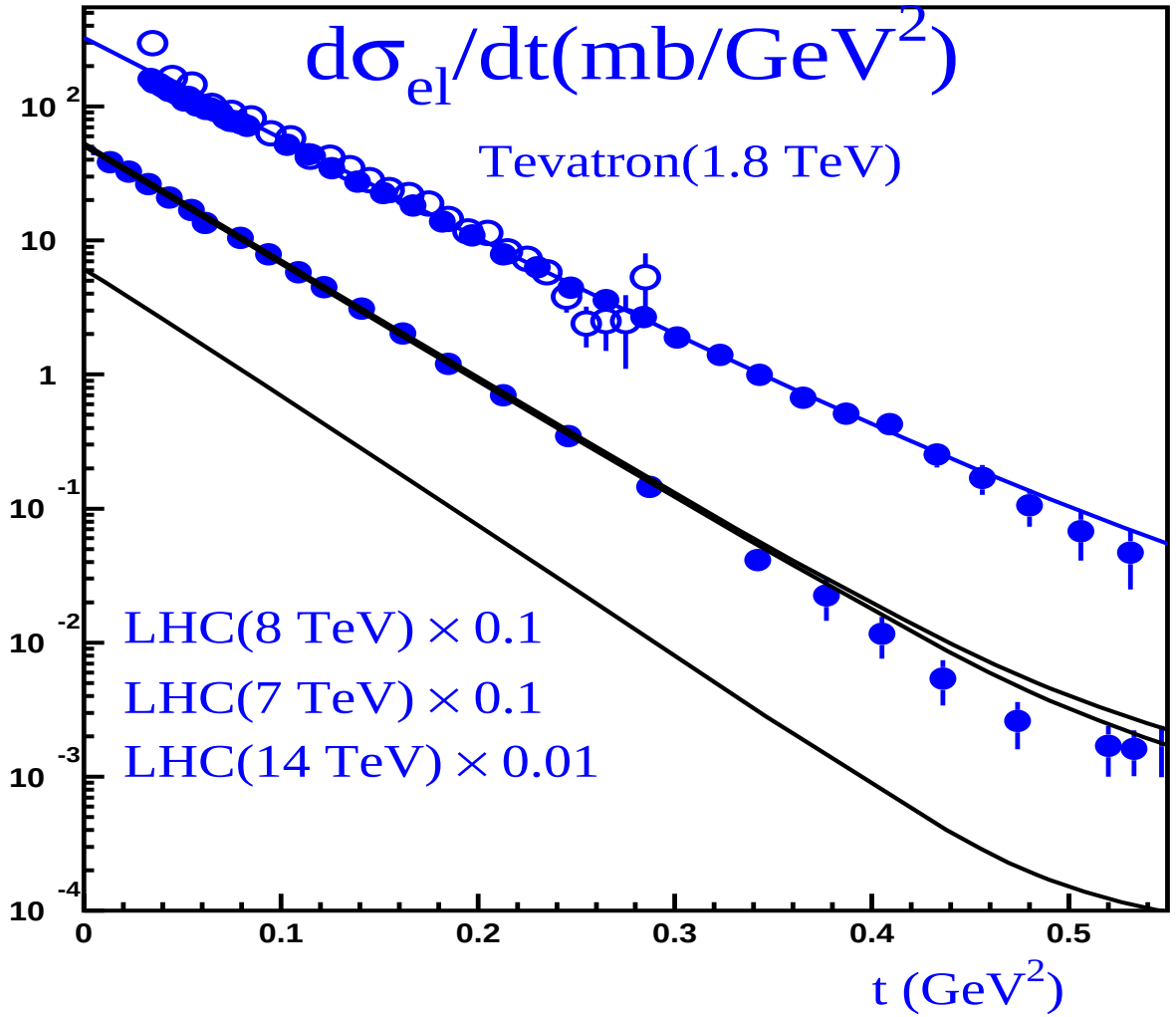

$d\sigma_{el}/dt$ versus $|t|$ at Tevatron (blue curve and data)) and LHC (black curve and data) energies ($W = 1.8\,TeV$, $8\,TeV$ and $7\,TeV$ respectively) The solid line without data shows our prediction for $W = 14\,TeV$.

From Ciesielski and Goulianos "MBR MC Simulation" arXiv:1205.1446

The $\sigma_{\rm tot}^{p^{\pm}p}(s)$ cross sections at a pp center-of-mass-energy $\sqrt{s}$ are calculated as follows:

$$\sigma_{\rm tot}^{p^{\pm}p} = \begin{cases} 16.79 s^{0.104} + 60.81 s^{-0.32} \mp 31.68 s^{-0.54} & \text{for } \sqrt{s} < 1.8 \text{ TeV}, \\ \sigma_{\rm tot}^{\rm CDF} + \frac{\pi}{s_0}\left[\left(\ln\frac{s}{s_F}\right)^2 - \left(\ln\frac{s^{\rm CDF}}{s_F}\right)^2\right] & \text{for } \sqrt{s} \geq 1.8 \text{ TeV}, \end{cases}$$

The energy at which "saturation " occurs $\sqrt{s_F} = 22$ GeV, and $s_0 = 3.7 \pm 1.5\, GeV^2$.

Their "event generator" follows Dino's "renormalized Regge-theory" model, and their numbers are based on the MBR-enhanced PYTHIA8 simulation.

Kaidalov and Poghosyan

"Description of soft diffraction in the framework of Reggeon calculus. Predictions for LHC" (arXiv:0909.5156)

Attempt to describe data on soft diffraction taking into account all possible non-enhanced absorptive corrections to 3 Reggeon vertices and loop diagrams.

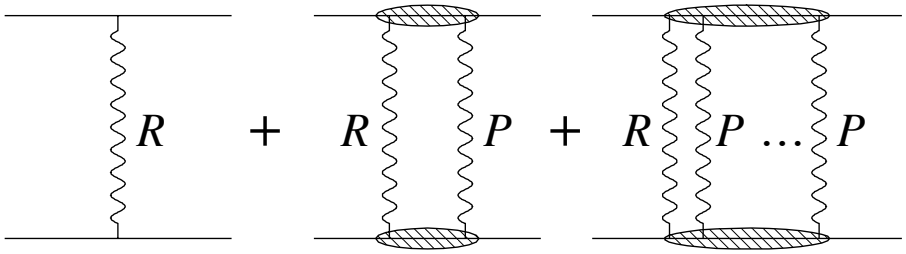

Figure 1: Single pole and RP^n cut contribution in the elastic scattering amplitude. R stands for secondary Reggeon and for Pomeron.

They apply AGK rules for calculating the discontinuity of the matrix element, and the generation of the optical theorem for the case of multi Pomeron exchange.

It is a single $I\!P$ model and with secondary Regge poles, they have $\Delta_{I\!P} = 0.12$; $\alpha'_{I\!P} = 0.22 GeV^{-2}$.

Results of Kaidalov and Poghosyan

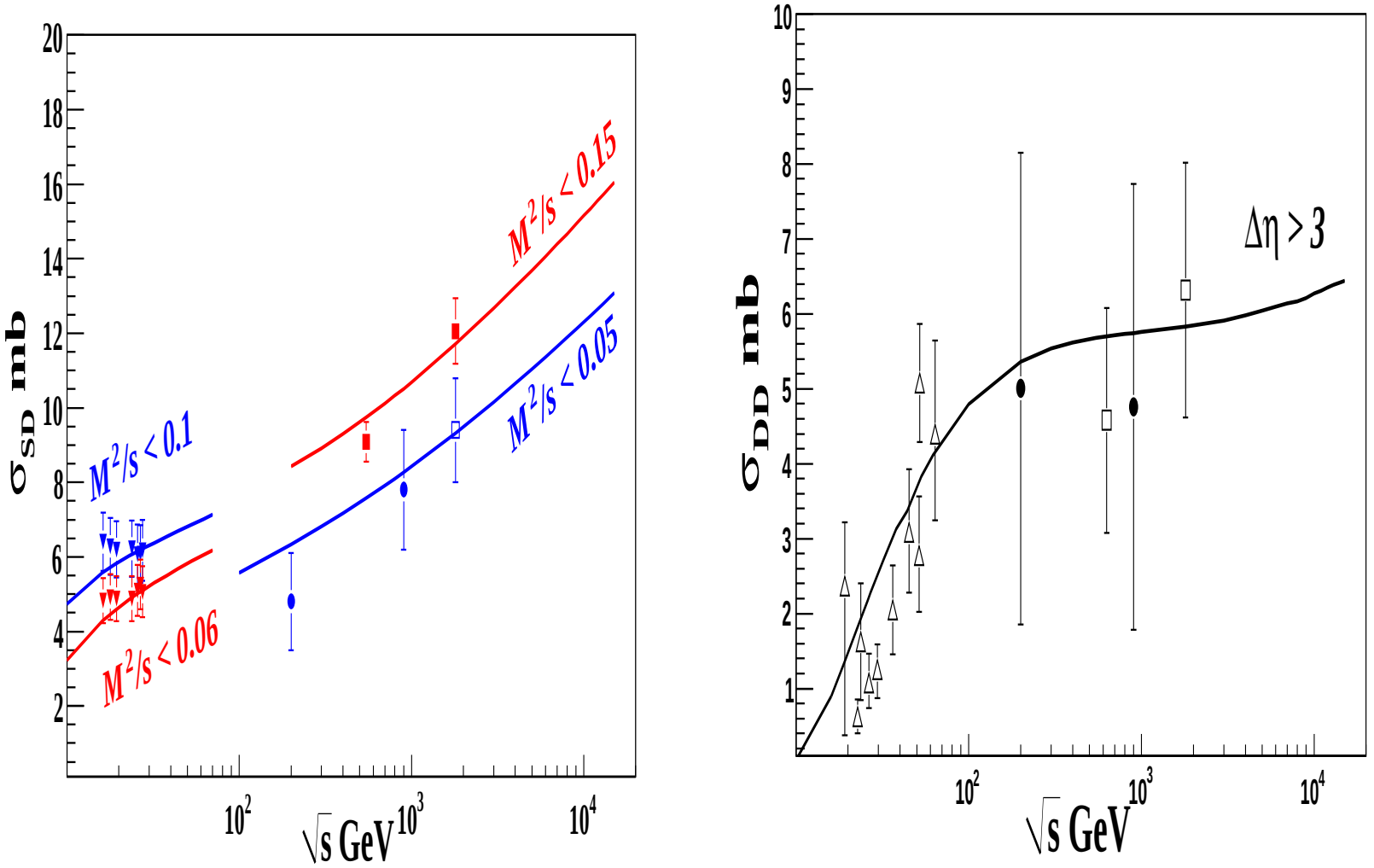

Figure 2: Integrated single and double diffractive cross-sections as a function of $\sqrt{s}$

Comparison of results obtained in GLM, Ostapchenko, K-P and KMR models

Ostapchenko (Phys.Rev.D81,114028(2010)) [pre LHC] has made a comprehensive calculation in the framework of Reggeon Field Theory based on the resummation of both enhanced and semi-enhanced Pomeron diagrams.
To fit the total and diffractive cross sections he assumes TWO POMERONS: (for SET C)

"SOFT POMERON" $\alpha^{Soft} = 1.14 + 0.14t$

"HARD POMERON" $\alpha^{Hard} = 1.31 + 0.085t$

The Durham Group (Khoze, Martin and Ryskin),(Eur.Phys.J.,C72(2012), 1937), to be consistent with the Totem result, have a model, based on a THREE channel eikonal description, with 3 diffractive eigenstates of different sizes, but with ONLY ONE POMERON.
$\Delta_{I\!P} = 0.14$; $\alpha'_{I\!P} = 0.1\ \ GeV^{-2}$. We will refer to this as KMR3C.

Recently KMR (arXiv:1306.2149) suggested a TWO channel eikonal model where the Pomeron couplings to the diffractive eigenstates depend on the collider energy. They have four versions of the model. The parameters of the Pomeron of their "favoured version" Model 4 are:
$\Delta_{I\!P} = 0.11$; $\alpha'_{I\!P} = 0.06\ \ GeV^{-2}$. We will refer to this as KMR2C.

Comparison of results of various models

W = 1.8 TeV	GLM	KMR3C	KMR2C	Ostap(C)	BMR*	KP
$\sigma_{\rm tot}(mb)$	79.2	79.3	77.2	73.0	81.03	75.0
$\sigma_{\rm el}(mb)$	18.5	17.9	17.4	16.8	19.97	16.5
$\sigma_{SD}(mb)$	11.27	5.9(LM)	2.82(LM)	9.2	10.22	10.1
$\sigma_{DD}(mb)$	5.51	0.7(LM)	0.14(LM)	5.2	7.67	5.8
$B_{el}(GeV^{-2})$	17.4	18.0	17.5	17.8		

W = 7 TeV	GLM	KMR3C	KMR2C	Ostap(C)	BMR	KP
$\sigma_{\rm tot}(mb)$	98.6	97.4	96.4	93.3	98.3	96.4
$\sigma_{\rm el}(mb)$	24.6	23.8	24.0	23.6	27.2	24.8
$\sigma_{SD}(mb)$	14.88	7.3(LM)	3.05(LM)	10.3	10.91	12.9
$\sigma_{DD}(mb)$	7.45	0.9(LM)	0.14(LM)	6.5	8.82	6.1
$B_{el}(GeV^{-2})$	20.2	20.3	19.8	19.0		19.0

W = 14 TeV	GLM	KMR3C	KMR2C	Ostap(C)	BMR	KP
$\sigma_{\rm tot}(mb)$	109.0	107.5	108.	105.	109.5	108.
$\sigma_{\rm el}(mb)$	27.9	27.2	27.9	28.2	32.1	29.5
$\sigma_{SD}(mb)$	17.41	8.1(LM)	3.15(LM)	11.0	11.26	14.3
$\sigma_{DD}(mb)$	8.38	1.1(LM)	0.14(LM)	7.1	9.47	6.4
$B_{el}(GeV^{-2})$	21.6	21.6	21.1	21.4		20.5

Comparison with other experiments and models

From van-der-Meer scan

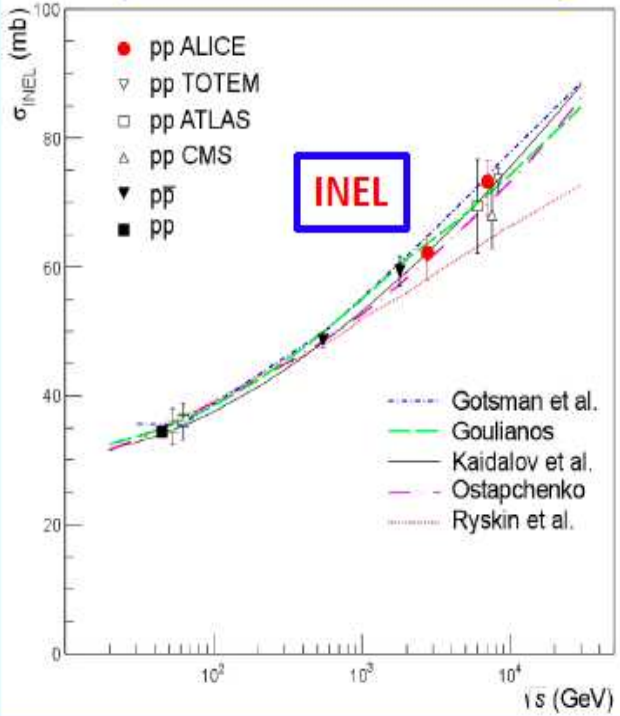

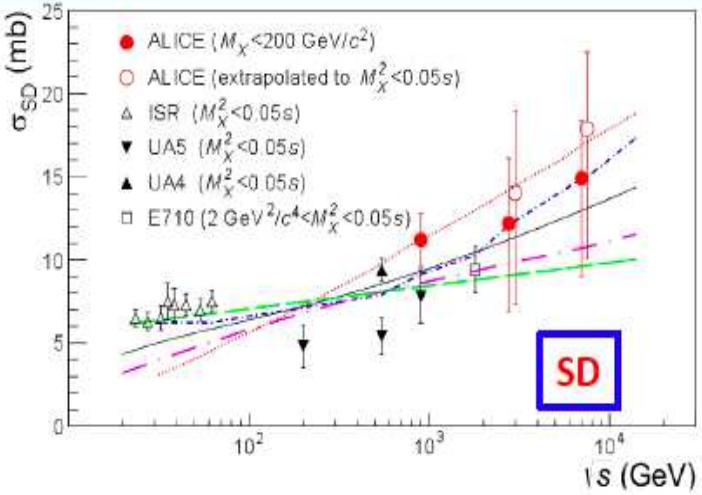

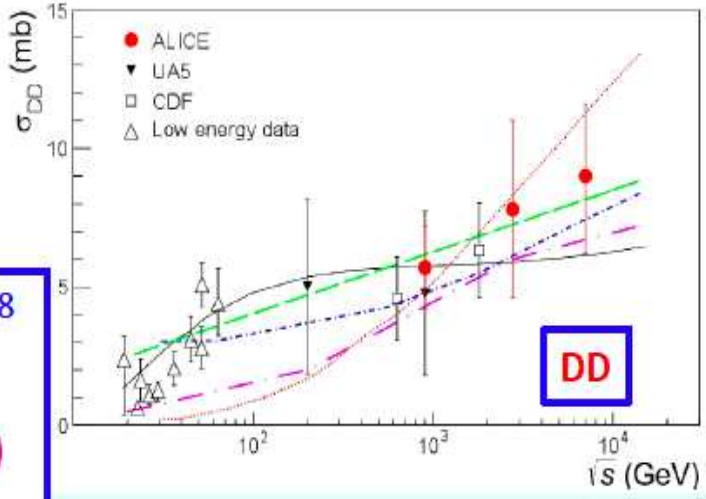

Gotsman et al. Phys. Rev. **D85** (2012), arXiv:1208:0898
Goulianos Phys. Rev. D80 (2009) 111901
Kaidalov et al., arXiv:0909.5156, EPJ **C67** 397 (2010)
Ostapchenko, arXiv:1010.1869, PR **D81** 114028 (2010)
Ryskin et al., EPJ **C60** 249 (2009), **C71** 1617 (2011)

Comparison of the results of GLM model and data at 7 and 57 TeV

W	σ_{tot}^{model}(mb)	σ_{tot}^{exp}(mb)	σ_{el}^{model}(mb)	σ_{el}^{exp}(mb)
7 TeV	98.6	TOTEM: 98.6 $\pm$2.2	24.6	TOTEM: 25.4$\pm$1.1

W	$\sigma_{in}^{model}(mb)$	σ_{in}^{exp}(mb)	$B_{el}^{model}(GeV^{-2})$	$B_{el}^{exp}(GeV^{-2})$
7 TeV	74.0	CMS: 68.0$\pm 2^{syst} \pm 2.4^{lumi} \pm 4^{extrap}$ ATLAS: 69.4$\pm 2.4^{exp} \pm 6.9^{extrap}$ ALICE: 73.2 $(+2./-4.6)^{model} \pm 2.6^{lumi}$ TOTEM: 73.5 $\pm 0.6^{stat} \pm 1.8^{syst}$	20.2	TOTEM: 19.9$\pm$0.3

W	$\sigma_{sd}^{model}(mb)$	σ_{sd}^{exp}(mb)	σ_{dd}^{model}(mb)	σ_{dd}^{exp}(mb)
7 TeV	$10.7^{GW} + 4.18^{nGW}$	ALICE : 14.9(+3.4/-5.9)	$6.21^{GW} + 1.24^{nGW}$	ALICE: 9.0 $\pm$ 2.6

W	σ_{tot}^{model}(mb)	σ_{tot}^{exp}(mb)
57 TeV	130	AUGER*: 133 $\pm 13^{stat} \pm 17^{sys} \pm 16^{Glauber}$
	σ_{inel}^{model}(mb)	σ_{inel}^{exp}(mb)
	95.2	AUGER*: 92 $\pm 7^{stat} \pm 11^{syst} \pm 7^{Glauber}$

*AUGER collaboration Phys.Rev.Lett.109,062002 (2012)

Conclusions

- We have succeded in building a model for soft interactions at high energy, which provides a very good description all high energy data, including the LHC measurements.
  This model is based on the Pomeron with a large intercept ($\Delta_{I\!P} = 0.23$) and very small slope ($\alpha'_{I\!P}$ =0.028).

- We find no need to introduce two Pomerons: i.e. a soft and a hard one.
  The Pomeron in our model provides a natural matching with the hard Pomeron in processes that occur at short distances.

- Amplitudes provide useful information but are NOT unique, and we require more accurate data to pin them down.

- The qualitative features of our model are close to what one expects from N=4 SYM, which is the only theory that is able to treat long distance physics on a solid theoretical basis.

M^2 distribution: data

➔ $d\sigma/dM^2|_{t=-0.05}$ ~ independent of s over 6 orders of magnitude!

Regge → data

$$\frac{d\sigma}{dM^2} \propto \frac{s^{2\varepsilon} \to 1}{(M^2)^{1+\varepsilon}}$$

Independent of s over 6 orders of magnitude in M^2

➔ M^2 scaling

KG&JM, PRD 59 (1999) 114017

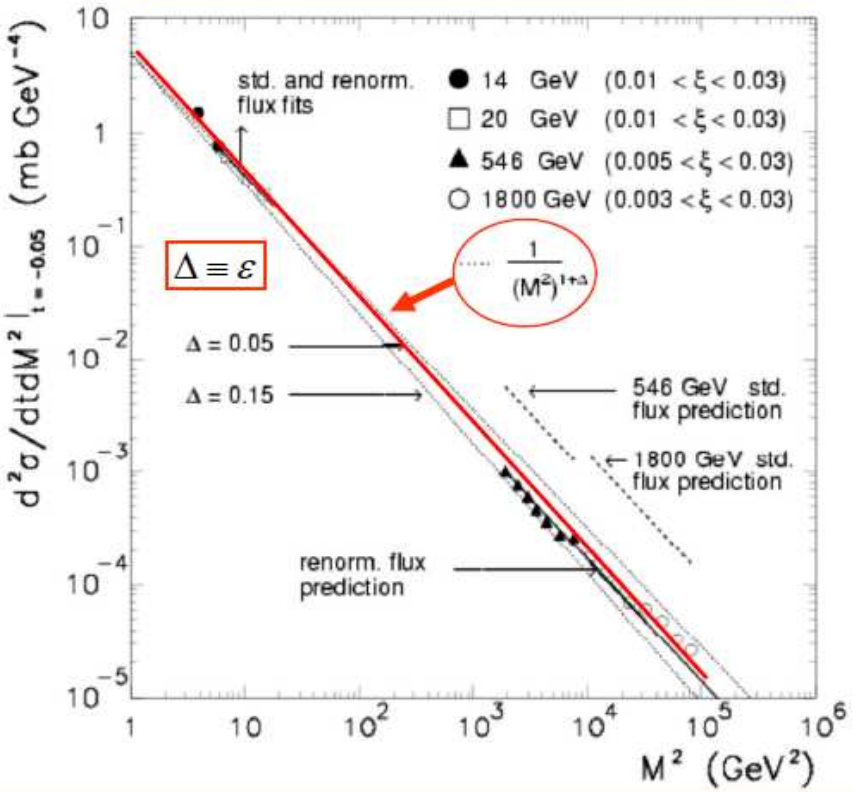

➔ factorization breaks down to ensure M^2 scaling

Modeling SD mass distributions

How do we account for diffracted masses (M_X) outside the detector acceptance?

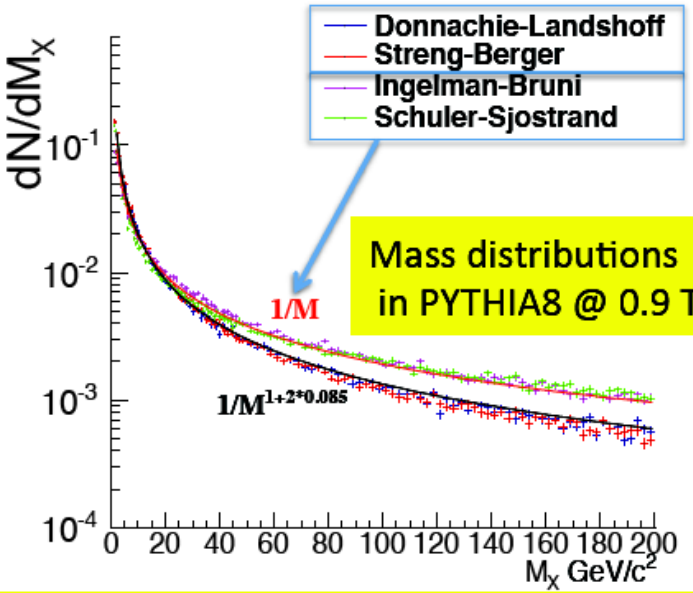

Mass distributions in PYTHIA8 @ 0.9 TeV

The systematic uncertainty estimated by ALICE was obtained from the Kaidalov-Poghosyan (KP) model with a ± 50% variation (grey area) and the Donnachie-Landshoff model, resulting into an asymmetric systematic error

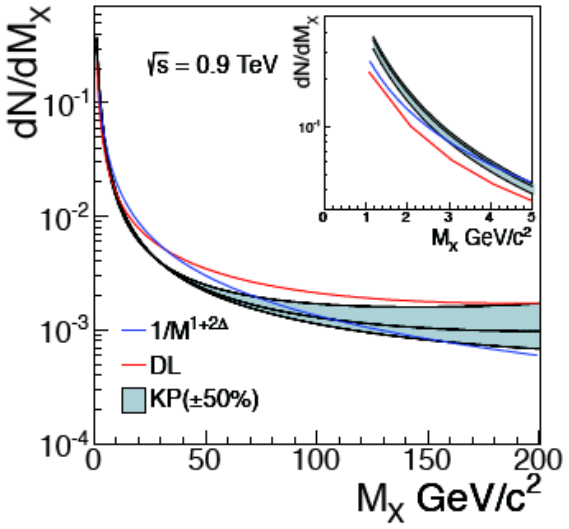

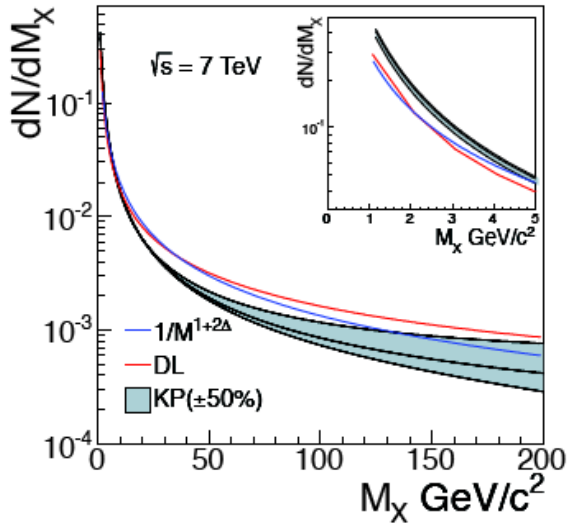

11

Measurement of σ_{INEL}

- Rate of MB_{AND} (coincidence between V0-L and V0-R) measured in a van der Meer scan

$$\frac{dN(MB_{AND})}{dt} = A \times \sigma_{INEL} \times L$$

$$A \times \sigma_{INEL} = 54.34 \pm 1.9 mb$$

- A = MB_{AND} efficiency obtained as described previously

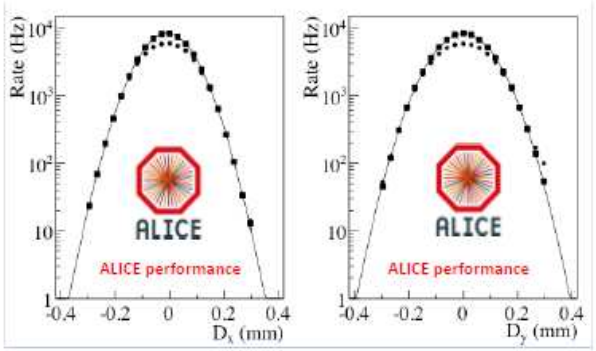

ALICE $\sigma_{INEL}(7TeV) = 73.2^{+2}_{-4.6}(\text{mod.}) \pm 2.6(lumi.)mb$

ATLAS : $69.4 \pm 2.4^{\text{exp.}} \pm 6.9^{\text{extr.}}$

CMS : $68.0 \pm 2.0^{\text{syst.}} \pm 2.4^{\text{lumi}} \pm 4^{\text{extr.}}$

TOTEM: $73.5 \pm 0.6^{\text{stat.}} {}^{+1.8}_{-1.3}{}^{\text{syst.}}$

Using PYTHIA8 (DL?) instead of our tuned MC we obtain:
σ_{INEL} = 68.5 ± 2.5 mb, very close to CMS and ATLAS numbers

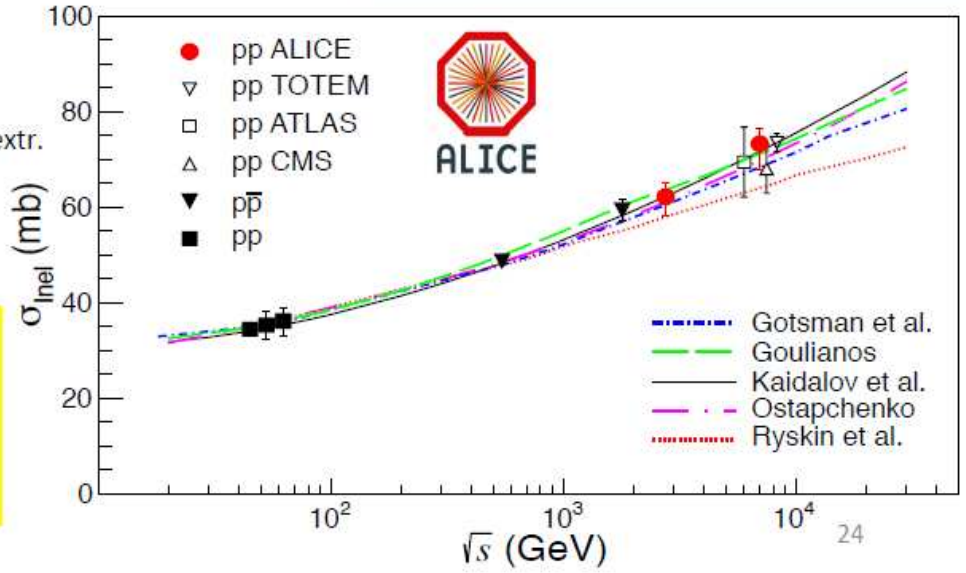

24

Soft diffractive cross sections

SD and DD cross sections (bin-by-bin correction)

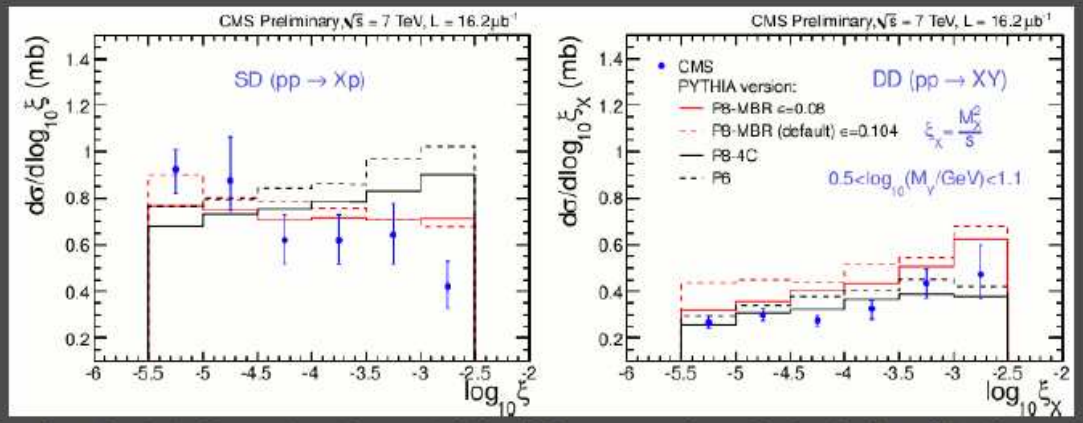

$$\frac{d\sigma^{SD}}{d\log_{10}\xi} = \frac{N^{data}_{noCASTOR} - (N_{DD} + N_{CD} + N_{ND})^{MC}}{acc \cdot \mathcal{L} \cdot (\Delta \log_{10}\xi)_{bin}}$$

$$\frac{d\sigma^{DD}}{d\log_{10}\xi_X} = \frac{N^{data}_{CASTOR} - (N_{ND} + N_{SD} + N_{CD})^{MC}}{acc \cdot \mathcal{L} \cdot (\Delta \log_{10}\xi_X)_{bin}}$$

MC-based background subtraction (see previous slide).
acc – acceptance (pileup correction included, ~7%).
Hadron level – generated masses.

Error bars dominated by systematic uncertainties (HF energy scale and hadronization+diffraction model uncertainties dominate).

Results compared to predictions of theoretical models used in PYTHIA8-MBR, PYTHIA8-4C and PYTHIA6:

- PYTHIA8 MBR shown for two values of the Pomeron trajectory ($\alpha(t) = 1+\varepsilon+\alpha' t$), ε=0.08 and ε=0.104. Both describe the measured SD cross section well. The DD data favour the smaller value of ε.
- The Schuler&Sjostrand model used in PYTHIA8-4C and PYTHIA6 describes the DD cross section, but fails to describe the falling behavior of the SD data.

The SD cross section integrated over $-5.5 < \log_{10}\xi < -2.5$:
Multiplied by 2 to account for both pp → pX and pp → Xp processes.

$$\sigma^{SD}_{vis} = 4.27 \pm 0.04\ (stat.)\ ^{+0.65}_{-0.58}\ (syst.)\ mb$$

$12 < M_X < 394$ GeV

CMS PAS FSQ-12-005

Soft diffractive cross sections

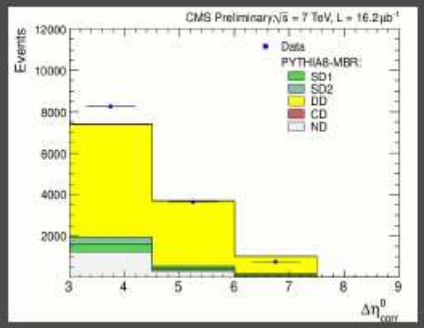

DD cross section with central LRG (bin-by-bin correction)

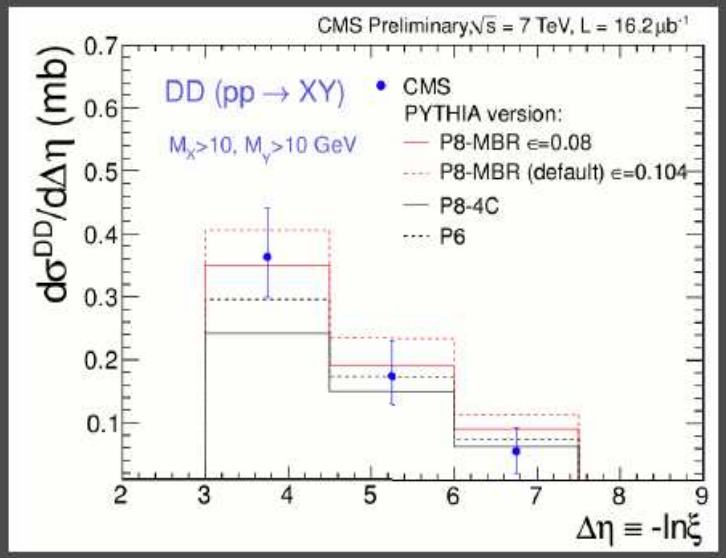

$$\frac{d\sigma^{DD}}{d\Delta\eta} = \frac{N^{data} - (N_{ND} + N_{SD} + N_{CD})^{MC}}{acc \cdot \mathcal{L} \cdot (\Delta\eta)_{bin}}$$

MC-based background subtraction, ND dominant.
acc – acceptance (pileup correction included, extrapolation from $\Delta\eta^0 > 3$ to $\Delta\eta > 3$) .
Hadron level – generated masses, $\Delta\eta = -\log(M_X^2 M_Y^2/ss_0)$.

Error bars dominated by systematic uncertainties (HF energy scale, and hadronization+diffraction model uncertainties dominate).

Results compared to predictions of theoretical models used in PYTHIA8-MBR, PYTHIA8-4C and PYTHIA6. The predictions are in agreements with the data.

The DD cross section integrated in the region $\Delta\eta > 3$, $M_X > 10$ GeV, $M_Y > 10$ GeV:

$$\sigma^{DD}_{vis} = 0.93 \pm 0.01\ (stat.)\ ^{+0.26}_{-0.22}\ (syst.)\ mb$$

DIS 2013, R. Ciesielski

CMS PAS FSQ-12-005 10

CMS SD and DD x-sections vs ALICE:

measurements and theory models

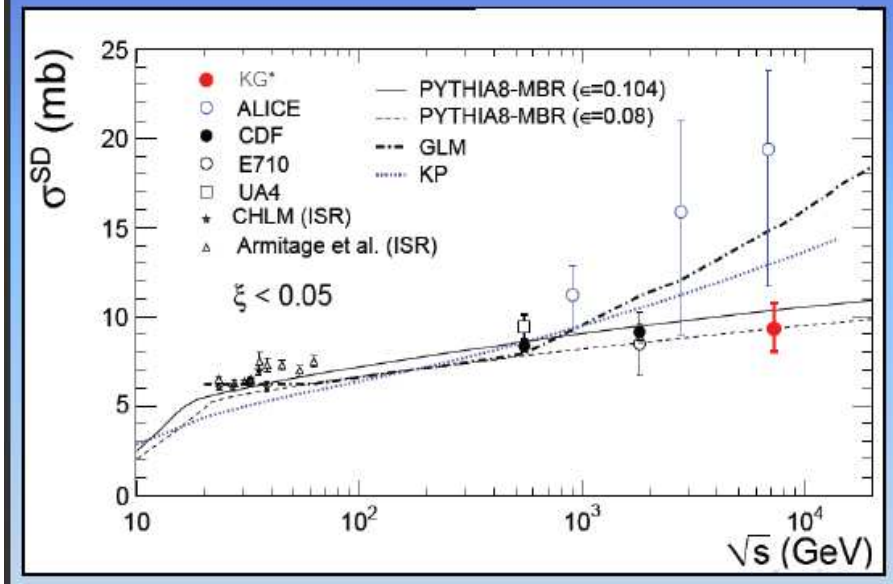

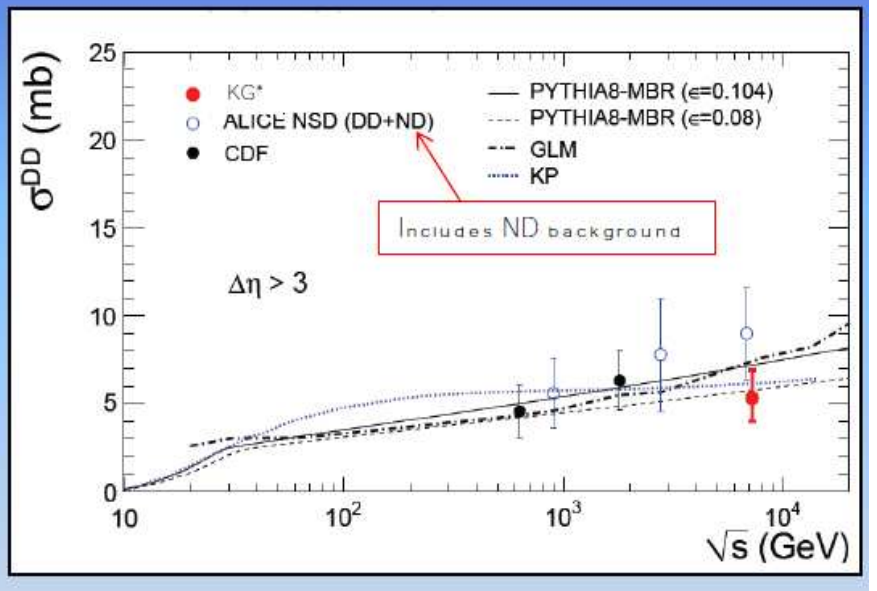

- KG*: after extrapolation into low ξ from measured CMS data using the MBR model:
  find details on data in Robert Ciesielski's talk on Wed. at 15:30.

Totem 8 TeV Data

8TeV cross sections

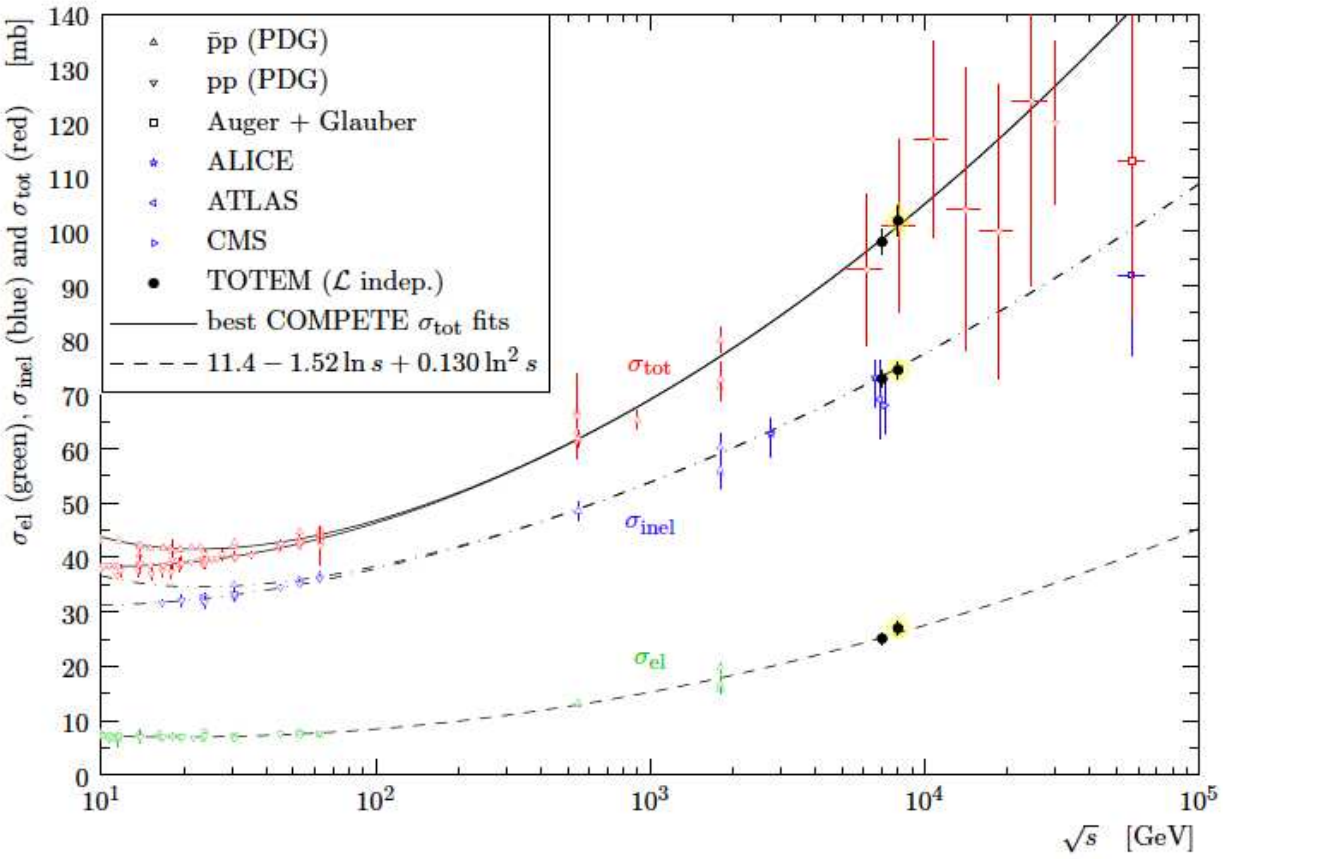

Nicola Turini 11 feb 2013

From Donnachie and Landshoff arXiv:1112.2485

D and L use an EIKONALIZED Regge pole model with Pomerons and Reggeons:

The values of the parameters are determined by making a simultaneous fit to pp scattering data and to DIS lepton scattering for low x.

Their results can be summarized:	SOFT POMERON	HARD POMERON
	$\alpha_S^{I\!P} = 1.093 + 0.25t$	$\alpha_H^{I\!P} = 1.362 + 0.1t$
Coupling strength:	$X_1 = 243.5$	$X_0 = 1.2$
At 7 TeV	σ_{tot}(soft) $= 91$ mb	σ_{tot}(hard + soft) $= 98$ mb

From Donnachie and Landshoff arXiv:1112.2485

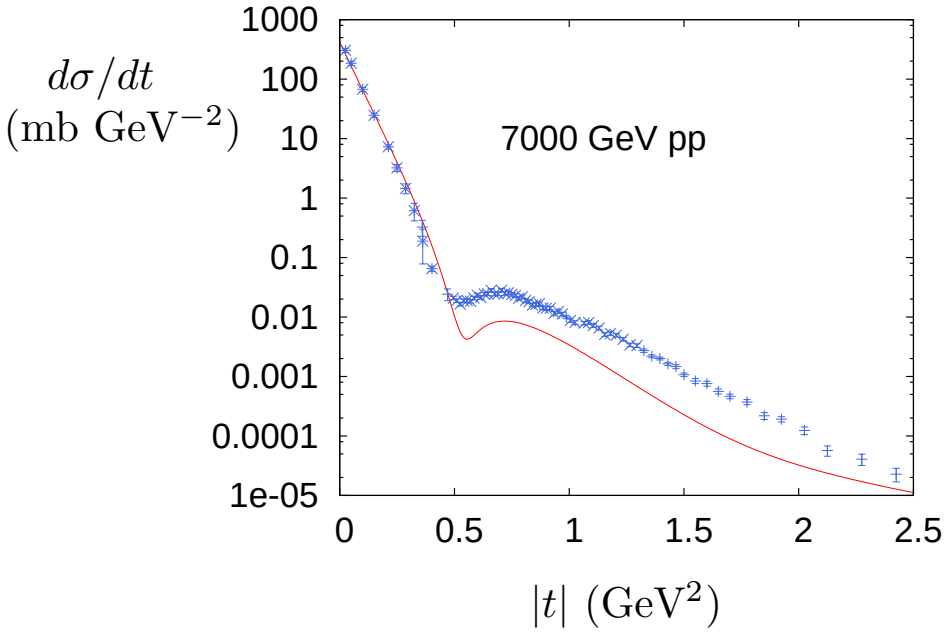

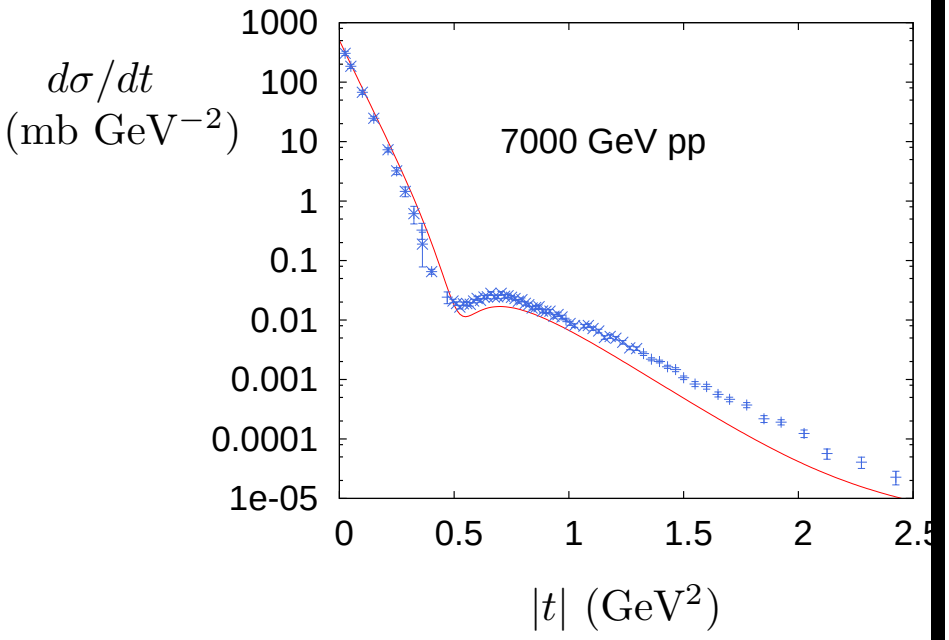

ONLY SOFT POMERON

(SOFT + HARD) POMERON

Block and Halzen's Parametrization of σ_{tot} and σ_{inel}

Bloch and Halzen (P.R.L. 107,212002 (2011) and arXiv:1205.5514) claim that the experimental data from LHC (at 7 Tev) and Auger (at 57 Tev), "saturate" the Froissart bound of $ln^2 s$. By "saturation" they mean that $\sigma_{tot} \approx ln^2 s$.

Using Analyticity constraints and in the spirit of FESR's they propose the following parametrization for the pp and p$\bar{p}$ cross sections:

$$\sigma_{tot} = 37.1(\frac{\nu}{m})^{-0.5} + 37.2 - 1.44ln(\frac{\nu}{m}) + 0.2817ln^2(\frac{\nu}{m})$$

$$\sigma_{inel} = 62.59(\frac{\nu}{m})^{-0.5} + 24.09 + 0.1604ln(\frac{\nu}{m}) + 0.1433ln^2(\frac{\nu}{m})$$

where ν denotes the lab energy, and at high energies $\nu = s/(2m$

W (Tev)	7	8	14	57
σ_{tot} mb	95.1 $\pm$ 1.1	97.6 $\pm$ 1.1	107.3 $\pm$ 1.2	134.8 $\pm$ 1.5
σ_{inel} mb	69.0 $\pm$ 1.3	70.3 $\pm$ 1.3	76.3 $\pm$ 1.4	92.9 $\pm$ 1.6

Diffractive Processes in our Formalism

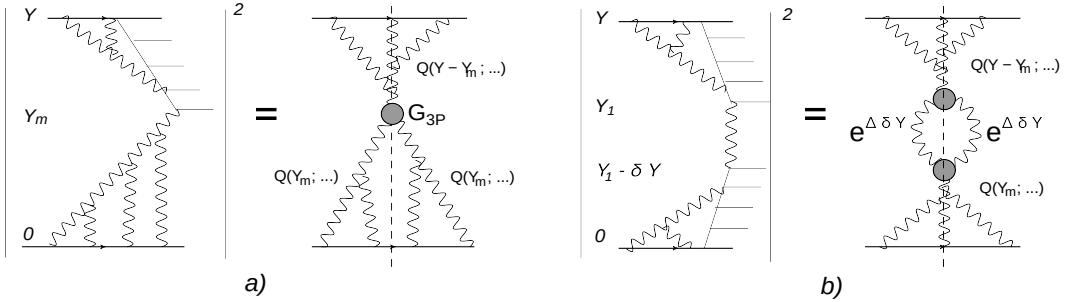

For diffraction production we introduce an additional contribution due to the Pomeron enhanced mechanism which is non GW.

As shown in fig-a, for (single diffraction) we have one cut Pomeron,

and in fig-b, for (double diffraction) we have two cut Pomerons

we express the cut Pomerons through a Pomeron without a cut, using the AGK cutting rules.

Fits to 57 TeV Data

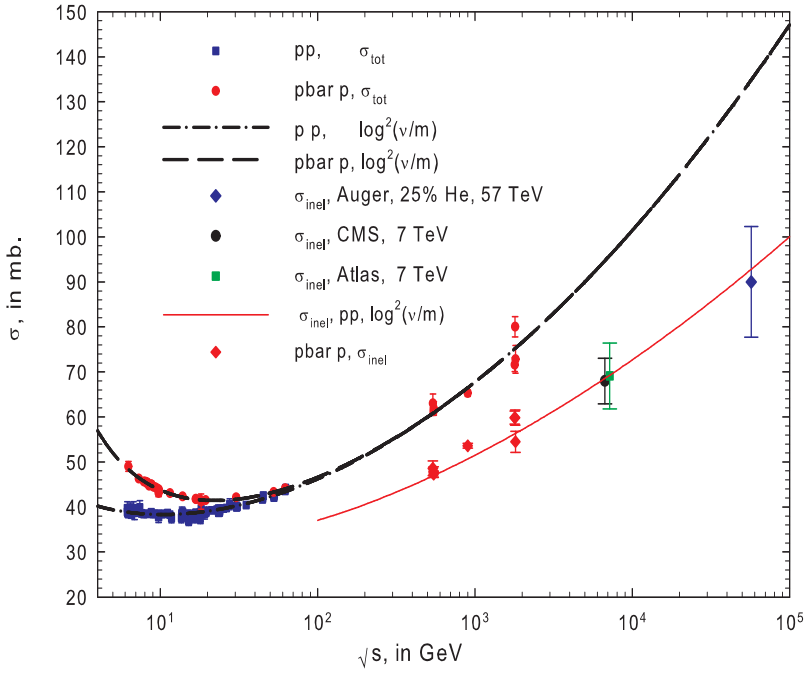

Block and Halzen parameterization

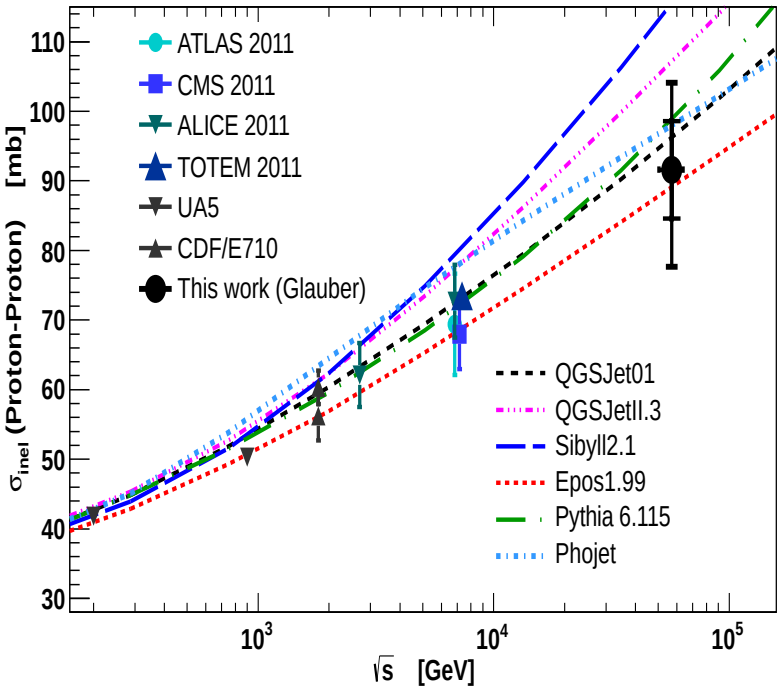

Auger Monte Carlo Fits

Guiding criteria for GLM Model

- The model should be built using Pomerons and Reggeons.
- The intercept of the Pomeron should be relatively large. In AdS/CFT correspondence we expect $\Delta_{I\!P} = \alpha_{I\!P}(0) - 1 = 1 - 2/\sqrt{\lambda} \approx 0.11$ to 0.33. The estimate for λ from the cross section for multiparticle production as well as from DIS at HERA is λ =5 to 9;
- $\alpha'_{I\!P}(0) = 0$;
- A large Good-Walker component is expected, as in the AdS/CFT approach the main contribution to shadowing corrections comes from elastic scattering and diffractive production.
- The Pomeron self-interaction should be small (of the order of $2/\sqrt{\lambda}$ in AdS/CFT correspondence), and much smaller than the vertex of interaction of the Pomeron with a hadron, which is of the order of λ;

Diffraction

For double diffraction we have (see Fig.1b):

$$A^{dd}_{i,k} = \int d^2b'\, 4\, g_i\left(\vec{b}-\vec{b}', m_i\right)\; g g_k\left(\vec{b}', m_k\right)$$
$$\times \quad Q\left(g_i, m_i, \vec{b}-\vec{b}', Y-Y_1\right)\; e^{2\Delta\,\delta Y}\, Q\left(g_k, m_k, \vec{b}', Y_1-\delta Y\right).$$

This equation is illustrated in fig-b, which displays all ingredients of the equation. We express each of two cut Pomerons through the Pomeron without a cut, using the AGK cutting rules. For single diffraction, $Y = \ln\left(M^2/s_0\right)$, where, M is the SD mass. For double diffraction, $Y - Y_1 = \ln\left(M_1^2/s_0\right)$ and $Y_1 - \delta Y = \ln\left(M_2^2/s_0\right)$, where M_1 and M_2 are the masses of two bunches of hadrons produced in double diffraction.

The integrated cross section of the SD channel is written as a sum of two terms: the GW term, which is equal to

$$\sigma^{GW}_{sd} = \int d^2b \left|\alpha\beta\{-\alpha^2\, A_{1,1} + (\alpha^2-\beta^2)\, A_{1,2} + \beta^2\, A_{2,2}\}\right|^2.$$

Diffraction 2

The second term describes diffraction production due to non GW mechanism:

$$\sigma_{sd}^{\rm nGW} = 2\int dY_m \int d^2b \tag{1}$$

$$\Big\{ \alpha^6 A^{sd}_{1;1,1} e^{-\Omega_{1,1}(Y;b)} + \alpha^2\beta^4 A^{sd}_{1;2,2} e^{-\Omega_{1,2}(Y;b)} + 2\,\alpha^4\,\beta^2\, A^{sd}_{1;1,2} e^{-\frac{1}{2}\left(\Omega_{1,1}(Y;b)+\Omega_{1,2}(Y;b)\right)}$$

$$+ \beta^2\,\alpha^4\, A^{sd}_{2;1,1} e^{-\Omega_{1,2}(Y;b)} + 2\,\beta^4\alpha^2\, A^{sd}_{2;1,2} e^{-\frac{1}{2}\left(\Omega_{1,2}(Y;b)+\Omega_{2,2}(Y;b)\right)} + \beta^6\, A^{sd}_{2;2,2} e^{-\Omega_{2,2}(Y;b)} \Big\}.$$

The cross section of the double diffractive production is also a sum of the GW contribution,

$$\sigma_{dd}^{GW} = \int d^2b\; \alpha^2\,\beta^2 \Big| A_{1,1} - 2\,A_{1,2} + A_{2,2}\Big|^2,$$

to which we add the term which is determined by the non GW contribution,

$$\sigma_{dd}^{\rm nGW} = \int d^2b \left\{ \alpha^4\, A^{dd}_{1,1}\, e^{-\Omega_{1,1}(Y;b)} + 2\alpha^2\,\beta^2 A^{dd}_{1,2}\, e^{-\Omega_{1,2}(Y;b)} + \beta^4\, A^{dd}_{2,2}\, e^{-\Omega_{2,2}(Y;b)} \right\}.$$

In our model the GW sector can contribute to both low and high diffracted mass, as we do not know the value of the typical mass for this mechanism, on the other hand, the non GW sector contributes only to high mass diffraction ($M_0^{nGW} \geq 20$ GeV).